Article:

eprints@whiterose.ac.uk
https://eprints.whiterose.ac.uk/

Title

On the gas permeability of the microporous layer used in polymer electrolyte fuel cells.

Authors

O. M. Orogbemi*, D.B. Ingham, M. S. Ismail, K. J. Hughes, L. Ma, M. Pourkashanian

Energy 2050, Department of Mechanical Engineering, Faculty of Engineering, University of Sheffield, Sheffield, S3 7RD, Sheffield. United Kingdom.

*Corresponding author, Tel: +44 114 215 7220

Email address: tomisinigbane@yahoo.com (O. M. Orogbemi)

Abstract

In an attempt to obtain accurate values of the gas permeability of the microporous layer (MPL), substrates with negligible MPL penetration and of known gas permeability, i.e. membrane filters, have been employed. The values of the MPL permeability obtained using the membrane filters were compared with those obtained conventionally using the carbon substrates. Due to MPL penetration, the MPL permeability obtained using the carbon substrate were found to decrease with carbon loading. On the other, due to negligible penetration, the MPL permeability obtained using the membrane filters were found to be almost invariant with the carbon loadings. Furthermore, the MPL permeability was found to be sensitive to the substrate used: more cracks (and subsequently substantially higher permeability) were shown by the MPLs coating the carbon substrates. This implies that the MPLs coating the carbon substrates and the MPLs coating the membrane filters are structure-wise different. It subsequently means that the MPL permeability obtained using the membrane filters cannot be used to estimate the MPL penetration into the carbon substrates.

Keyword: PEFCs; Microporous layer; Gas permeability; Penetration.

1. Introduction

A polymer electrolyte fuel cells (PEFC) is a promising clean power conversion technology as it has some very appealing features: high efficiency, rapid start-up and ease of manufacture [1-2.]. The gas diffusion layers (GDLs) play a crucial role in PEFCs. They are supposed to: distribute the reacting gases to the catalyst layer; remove excess liquid water away from the catalyst layer; act as an intermediate layer to transport electrons and heat between the catalyst layers and the flow-field plates [2-10]. The GDL is normally treated with a hydrophobic agent such as polytetrafluorethylene (PTFE) to enhance its ability to reject liquid water. The surface of the GDL facing the catalyst layer is also coated with a thin layer composed of carbon powder and PTEF particles to improve the contact with the catalyst layer and assist in removing liquid water from the cathode catalyst layer; this thin layer is called the microporous layer (MPL). The bare GDL, i.e. the GDL without the MPL, is often called the carbon substrate; the latter term will be used in this work. Notably, most of the modelling studies treat the carbon substrate and the MPL as a single component that normally has the characteristics of the carbon substrate [11, 20, 23, 25-27]. However, the relevant experimental studies have shown that the MPL has physical properties that are different to those of the carbon substrate by up to 2-3 orders of magnitudes [12]. Therefore, to have more predictive results from the modelled PEFCs, it is important to characterise the MPLs. Recognising this importance, there have been investigations to estimate, for example, the gas diffusivity [13-14, 16-17] and the thermal conductivity [17] of the MPLs.

For the two-phase modelled PEFCs, it is important to use accurate values for the permeability of the various porous layers in the membrane electrode assembly (MEA); the MEA is the heart of the fuel cell and typically consists of an electrode and GDL at each side of the fuel cell and a single polymeric membrane electrolyte at its centre. The permeability significantly affects the capillary diffusivity and consequently the saturation profile within the MEA [17]. The focus

3

of this work is to accurately estimate the gas permeability of the MPL. To achieve this, we need accurate estimation of the thickness of the MPL coating the carbon substrate. However, the MPL penetration into carbon substrate is significant [19, 22] and therefore the accurate estimation of the 'real' thickness of the MPL is a challenging task. The investigators normally assume that the difference in thicknesses, measured by a micrometer or estimated from cross-sectional images, before and after MPL coating is the thickness of the MPL [21, 24, 26]. Apparently, this approach incurs some inaccuracy in determining the MPL permeability and this is due to the MPL penetration mentioned above. To isolate the MPL penetration effects and subsequently accurately estimate the MPL permeability, one needs to use an appropriate porous substrate that is intolerant to penetration when applying the MPL ink; we have adopted this approach in this work. Specifically, the MPL permeability has been first determined conventionally using the carbon substrates and then determined using a membrane filter that has shown negligible penetration. The results have been then compared and contrasted. Furthermore, one would think that obtaining the accurate value of the MPL permeability will allow for the determination of the MPL penetration into the carbon substrate. This idea is explored in this work.

2. Materials and methods

Two commercial carbon black powders were considered in this study, namely Ketjenblack EC-300J MPL (AkzoNobel, the Netherlands) and Vulcan XC-72R (Cabot Corporation, USA). Table 1 summarises the physical properties of the carbon blacks as provided by the manufacturers. The carbon substrate used in this study was SGL 10BA (SGL Carbon GmbH, Germany). The physical properties of the SGL 10BA carbon substrate, as provided by the manufacturers, are listed in Table 2. A membrane filter, AAWP02500 (Merck Millipore, US), with a diameter of 25 mm, a thickness of 140 µm and pore size of 0.8 µm, was selected as a candidate substrate that allows negligible MPL penetration.

Five sets of MPL-coated GDL samples were prepared following the procedures available in [18, 22, 29]. In each set, there were 6 samples which share the same carbon loading in the MPLs. The carbon loadings considered were 0.5, 1.0, 1.5, 2.0 and 2.5 mg/cm^2. The MPL composition of all the carbon loadings by weight in the MPL ink has been kept unchanged: 80 % carbon black and 20 % PTFE. The hydrophobic agent used was 60 wt. % PTFE emulsion (Sigma-Aldrich, UK). The calculated amounts of the carbon black and the PTFE dispersion were manually mixed until a paste-like material was formed. Isopropyl alcohol was added, as a dispersion agent, to the formed mixture and the resulting slurry was sonicated until an ink with a good dispersion was formed. In this work, nitrogen gas is used for applying the ink slurry on the surfaces of the samples. The samples of the carbon substrates were made circular with a 2.50 cm diameter.

The thickness of the GDL and the membrane filter samples was measured before and after the MPL-coating using a micrometre which has an accuracy of 2.5 µm, in order to estimate thickness of the MPL. Each sample was measured at 4 equally-spaced positions within it to provide a well-estimated average value of the thickness. To confirm the thicknesses measured by the micrometre, SEM cross-section images were taken for some of the MPL-coated samples and the thickness of the MPL was visually estimated at as many points as possible and subsequently averaged. Further, the SEM cross-section images were used to confirm that there is negligible MPL penetration in the case of the membrane filter; see Fig. 1. The SEM images were produced using the scanning electron microscope JEOL (JBM-BO10LA).

2.1 Gas permeability setup

The experimental setup used in this work has been previously used in [18] for estimating the through-plane permeability of the GDLs; see Fig. 2. As shown in Fig. 2, the setup consists of

upper and lower fixtures, with the sample fixed between the two fixtures and nitrogen gas was the gas flowing through the sample. The pressure drop across the sample was measured at 8 equal-interval values of the flow rate. The flow controller used was an HFC-202 (Teledyne Hastings, UK) with a range of 0.0 – 0.5 SLPM and the differential pressure sensor used was a PX653 (Omega, UK) with a range of ±12.5 Pa.

[Insert Fig. 2]

2.2 Data analysis

Sufficiently low flow rates were used to render the inertial losses negligible and consequently Darcy's Law is employed [21]:

$$\frac{\Delta P}{L} = \frac{\mu}{k} V \tag{1}$$

$$V = \frac{Q}{\pi D^2/4} \tag{2}$$

where ΔP is the pressure drop across the sample, L is the thickness of the sample, μ is the dynamic viscosity of the nitrogen gas at the test temperature (~20 °C), k is the gas permeability of the porous sample, V is the velocity of the flowing gas, Q is the volumetric flow rate and D is the diameter of the sample exposed to the flow. Since the carbon substrate and MPL are typically layered in the coated GDLs, the pressure drop across the coated sample can be consequently expressed as follows [28]:

$$\Delta P_{tot} = \Delta P_{MPL} + \Delta P_{sub} \tag{3}$$

where ΔP_{tot}, ΔP_{MPL} and ΔP_{sub} are the pressure drops across the coated substrate, the MPL and the substrate, respectively. From Equation (1), Equation (3) can be written as follows:

$$\frac{\mu L_{tot}}{k_{tot}}V = \frac{\mu L_{MPL}}{k_{MPL}}V + \frac{\mu L_{sub}}{k_{sub}}V \qquad (4)$$

where L_{tot}, L_{MPL} and L_{sub} are the thicknesses of the coated substrate, the MPL and the carbon substrate, respectively, and k_{tot}, k_{MPL} and k_{sub} are the gas permeability coefficients for the coated substrate, the MPL and the carbon substrate, respectively. Assuming that there is no MPL penetration into the substrate (as is typically the case for the membrane filters), one can make use of Equation (4) to determine the permeability of the MPL:

$$K_{MPL} = \frac{L_{MPL}}{\frac{L_{tot}}{K_{tot}} - \frac{L_{sub}}{K_{sub}}} \qquad (5)$$

As mentioned in the introduction, the MPL penetration into the carbon substrates is significant. Assuming that the penetration part of the MPL has the same characteristics as the pure MPL, Equation (5) can be slightly modified in order to account for the MPL penetration which is represented in the below equation by the symbol L_{pen}:

$$K_{MPL} = \frac{L_{MPL} + L_{pen}}{\frac{L_{tot}}{K_{tot}} - \frac{L_{sub} - L_{pen}}{K_{sub}}} \qquad (6)$$

Fig. 3 shows a schematic diagram for the cross-section of the MPL-coated GDL in which a distinction has been made between the visible thickness of the MPL and the MPL penetration.

[Insert Fig. 3]

3. Results and discussion

The permeability of the MPL has been first estimated assuming that the MPL penetration into the carbon substrate is neglected and Equation (5) was used to calculate the permeability of the MPL [18]. As mentioned in Section 2, the thickness of the carbon substrate before (L_{sub}) and after (L_{tot}) MPL-coating were measured using a micrometre. The difference between the two thicknesses was assumed to be the thickness of the MPL (L_{MPL}). The permeability of the bare (k_{sub}) and MPL-coated carbon substrate (k_{tot}) were estimated using Equation (1). The viscosity value used was that of nitrogen at 20 °C, namely 1.76×10^{-5} Pa s. With all the above information, one can calculate the gas permeability of the MPL; as an example, Table 3 shows the values used to calculate the gas permeability of the MPL for the Ketjenblack carbon black and 2.0 mg/cm^2 carbon loading.

Fig. 4 shows the average values for the MPL permeability for all the carbon loadings of the 2 carbon blacks; the permeability values have been already estimated in a previous work [18]. The figure shows that, for both carbon blacks used, there is a general decline in the permeability of the MPL as the carbon loading increases. This must not be the case as the composition of the MPL was the same for all the carbon loadings investigated, i.e. 80 % carbon black and 20 % PTFE, and therefore the permeability of the MPL for a given carbon black must remain invariant for all the carbon loadings. As pointed out in Section 2, the main culprit for such a trend is the MPL penetration into the carbon substrate.

[Insert Table 3 and Fig. 4]

Therefore, what is required to more accurately calculate the gas permeability of the MPL is to use a porous substrate which reasonably permeates the gas and also allows no MPL penetration; the candidate substrate was the membrane filter described in Section 2. As shown in Fig. 1, the MPL penetration is almost negligible. Having coated the membrane filter substrate and used

Equation (5), the MPL permeability was estimated with the Ketjenblack carbon black as $2.92\pm0.02 \times 10^{-13}$ m^2 and with the Vulcan carbon black as $4.30\pm0.01 \times 10^{-14}$ m^2. The values used to estimate the gas permeability of the MPLs of the membrane filters are shown in Table 4. To confirm that the permeability of the MPLs with the same composition does not vary with the carbon loading, two carbon loadings (i.e. 0.5 and 1.0 mg/cm^2) were used for the membrane filter substrates. The initial plan was to estimate the permeability of the MPL for all the carbon loadings. Unfortunately, this has not been possible as the coated membrane filters with carbon loadings beyond 1.0 mg/cm^2 were found to be highly fragile and brittle and therefore easily subject to breakage when placing them in the setup. For the considered 2 carbon loadings, the MPL gas permeability was found to be almost invariant with carbon loading; see Table 4.

[Insert Table 4]

Comparing the values of the MPL permeability obtained from the coated carbon substrates (Fig. 4) with those obtained from the coated membrane filters (Table 4), it can be seen that the MPL permeability calculated using the carbon substrates is higher than those obtained using the membrane filters by up to 2 orders of magnitude. The possible reason behind this is that the large pores at the surface of the carbon substrate facilitate a substantial penetration of the MPL material into the body of the carbon substrate; consequently, the surface of the carbon substrate is not fully covered with the MPL material, especially for relatively low carbon loading cases. Fig 5 clearly shows that, for a carbon loading of 0.5 mg/cm^2, the surface of the carbon substrate used has been hardly covered with the MPL material. The level of MPL coverage enhances as the carbon loading increases; this is evident from the relevant surface SEM images (an example is given in Fig 6) and also from the decrease in the MPL permeability with increasing carbon loading as shown in Fig 4. Apparently, for both carbon blacks, the MPL permeability starts to decrease less after the carbon loading 1-1.5 mg/cm^2. However, the minimum values of the MPL permeability obtained using the carbon substrates remain considerably higher than the

corresponding values of the MPL permeability obtained from the membrane filters. Fig. 7 shows that the surface of the MPL-coated membrane filter features less cracks than those of the MPL-coated substrates; this is most likely the reason that the MPL permeability obtained from carbon substrate are considerably higher than those obtained from membrane filters. The main culprit behind the availability of more cracks in case of carbon substrates is probably their superficial morphology which feature uneven surface and presence of large pores; see Fig.8.

As mentioned in the previous two sections, the initial thoughts were that the absence of the MPL penetration when using the membrane filters will allow one to accurately estimate the permeability of the MPL and subsequently possibly use it to estimate the MPL penetration into the carbon substrate. However, this is apparently not possible: the morphology of the MPL is sensitive to the substrate used for the MPL application; the carbon substrates impose more cracks in the MPL than the membrane filters. Therefore, we have structurally different MPLs and therefore the MPL permeability obtained from the membrane filters cannot be used to estimate the MPL penetration into the carbon substrate through using Equation (6) presented in Section 2.

[Insert Fig. 5-8]

4. Conclusions

Membrane filters with known gas permeability and negligible MPL penetration were used to accurately estimate the MPL permeability. For the purpose of comparison, the MPL permeability was also estimated conventionally using the carbon substrates. Two carbon blacks were used and various carbon loadings were investigated. The following are the main findings.

i. The MPL permeability obtained using the carbon substrates was found to decrease with carbon loading, though the same composition was used for all the carbon loadings. This was attributed to the MPL penetration into the carbon substrates.

ii. The MPL permeability obtained using the membrane filters was found to remain almost constant with the two investigated carbon loadings. This was attributed to the absence of MPL penetration

iii. The MPL permeability obtained using the carbon substrates was shown to be higher than that obtained using the membrane filters by up to 2 orders of magnitudes. The difference between the MPL values obtained from the two substrates becomes smaller as the carbon loading increases. These two observations were attributed to the incomplete MPL coverage of the surface of the carbon substrate (mainly for the low carbon loadings) and/or the presence of more cracks in the MPLs coating the carbon substrates (mainly for the high carbon loadings).

iv. Due to sensitivity of the MPL to the substrate used, the MPL obtained using the membrane filters cannot be used to estimate the MPL penetration into the carbon substrates.

Acknowledgements

References

[1]   T. Kitahara, T. Konomi, H. Nakajima, Microporous layer coated gas diffusion layers for enhanced performance of polymer electrolyte fuel cells J. Power Sources 195 (2010) 2202-2210.

[2]   V. Gurau, M. J. Bluemle, E. S. De Castro, Y. M. Tsou, T. A. Zawodzinski, Jr., J. A. Mann Jr., Characterization of transport properties in gas diffusion layers for proton exchange membrane fuel cells 2. Absolute permeability, J. Power of Sources 165 (2007) 793-802.

[3]   E.Antolini, R. R. Passos, E. A. Ticianelli, Effects of the carbon powder characteristics in the cathode gas diffusion layer on the performance of polymer electrolyte fuel cells, J. Power Sources 109 (2002) 477- 482.

[4]   C. J. Tseng, S. K. Lo, Effects of microstructure characteristics of gas diffusion layer and microporous layer on the performance of PEMFC, Energy Conversion and Management 51 (2010) 667-684.

[5]   M. Prasanna, H. Y. Ha, E. A. Cho, S,-A. Hong, H. –H. Oh, Influence of cathode gas diffusion media on performance of the PEMFCs, J. Power of Sources 131 (2004) 147-154.

[6]   D. Shou, Y. Tang, L. Ye, J. Fan, F. Ding, Effective permeability of gas diffusion layer in proton exchange membrane fuel cells, Int. J. Hydrogen Energy 38 (2013) 10519-10526.

[7]   R. P. Ramasamy, E. C. Kumbur, M. M. Mench, W. Liu, D. Moore, M. Murthy, Investigation of micro- and macro-porous layer interaction in polymer electrolyte fuel cells, Int. J.   Hydrogen Energy 33 (2008) 3351-3367.

[8]   S. Park, J. –W. Lee, B. N. Popov, A review of gas diffusion layer in PEM fuel cells: materials and designs, Int. J. Hydrogen Energy 37 (2012) 5850-5865.

[9]   G. Lin, T. V. Nguyen, Effect of thickness and hydrophobic polymer content of the gas diffusion layer on electrolyte flooding level in a PEMFC, J. The Electrochemical Society 152 (2005) A1942-A1948.

[10]   R. K. Phillip, B. R. Friess, A. D. Hicks, J. Bellerive, M. Hoorfar, Ex-situ measurement of properties of gas diffusion layers of PEM fuel cells, Energy Procedia 29 (2012) 486-495.

[11]   A. Z. Weber, J. Newman, Effects of microporous layers in polymer electrolyte fuel cells, J. Electrochemical Society152 (2005) A677-A688.

[12]   M. S. Ismail, D. B. Ingham, K. J. Hughes, L. Ma, M. Pourkashanian, Effect of diffusivity of polymer electrolyte fuel cell gas diffusion layers: An overview and numerical study, Int. J. Hydrogen Energy 40 (2015) 10994-11010.

[13]   C. Chan, N. Zamel, X. Li, J. Shen, Experimental measurement of effective diffusion coefficient of gas diffusion layer/microporous layer in PEM fuel cells, Electrochimica Acta 65 (2012) 13-21.

[14]   A. Nanjundapa, A. S. Alavijeh, M. E. Hannach, D. Harvey, E. Kjeang, A customeized framework for 3-D morphological characterization of microporous layers, Electrochemica Acta 110 (2013) 349-357.

[15]   F. Zabihian, A. S. Fung, Performance analysis of hybrid solid oxide fuel cell and gas turbine cycle (part I): Effects of fuel composition on output power, J. Energy Institute 87 (2014) 18 – 27.

[16]   X. Zhang, Y. Gao, H. Ostadi, K. Jiang, R. Chen, Modelling water intrusion and oxgen diffusion in a reconstructed microporous layer of PEM fuel cells, Int. J. Hydrogen Energy 39 (2014) 17222-17230.

[17]   O. S. Burheim, G. A. Crymble, R. Bock, N Hussain, S. Pasupathi, A. D. Plessis, S. L. Roux, F. Seland, H. Su, B. G. Pollet, Thermal conductivity in the thress layered regions of micro porous layer coated porous transport layers for the PEM fuel cell, Int. J. Hydrogen Energy 40 (2015) 16775-16785.

[18]   O. M. Orogbemi, D. B. Ingham, M. S. Ismail, K. J. Hughes, L. Ma, M. Pourkashanian, through-plane gas permeability of gas diffusion layers and microporous layer: effects of carbon loading and sintering, J. Energy Institute (2017) 1-9.

[19]   M. S. Ismail, D. Borman, T. Damjanovic, D. B. Ingham, M. Pourkashanian, On the through-plane permeability of microporous layer-coated gas diffusion layers used in proton exchange membrane fuel cells, Int. J. Hydrogen Energy 36 (2011) 10392-10402.

[20]   G. Hu, G. Li, Y. Zheng, Z. Zhang, Y. Xu, Optimization and parametric analysis of PEMFC based on an agglomerate model for catalyst layer, J. Energy Institute 87 (2014) 163 – 174.

[21]   O. M. Orogbemi, D. B. Ingham, M. S. Ismail, K. J. Hughes, L. Ma, M. Pourkashanian, The effects of the composition of microporous layers on the permeability of gas diffusion layers used in polymer electrolyte fuel cells, Int. J. Hydrogen Energy 41 (2016) 21345-21351.

[22]   S. Park, J. W. Lee, B. N. Popov, Effect of carbon loading in microporous layer on PEM fuel cell performance, J. Power Sources 163 (2006) 357-363.

[23]   E. Afshari, M. Ziaei-Rad, M. M. Dehkordi, Numerical investigation on a novel zigzag-shaped flow channel design for cooling plates of PEM fuel cells, J. Energy Institute (2016) 1-12.

[24]   T. Kitahara, T. Konomi, H. Nakajima, Microporous layer coated gas diffusion layers for enhanced performance of polymer electrolyte fuel cells, J. Power Sources 195 (2010) 2202-2210.

[25]   S. Subramanian, G. Rajaram, K. Palaniswamy, V. R. Jothi, Comparison of perforated and serpentine flow fields on the performance of proton exchange membrane fuel cell, J. Energy Institute (2016) 1-9.

[26]   E. Carcadea, H. Ene, D.B. Ingham, R. Lazar, L. Ma, M. Pourkashanian, I. Stefanescu, A computational fluid dynamics analysis of a PEM fuel cell system for power generation, Int. J. Numerical Methods Heat Fluid Flow 17 (2007) 302–312.

[27]   S. Subramanian, G. Rajaram, K. Palaniswamy, V. R. Jothi, Comparison of perforated and serpentine flow fields on the performance of proton exchange membrane fuel cell, J. Energy Institute (2016) 1-9.

[28]   T. H. Ko, W. S. Kuo, S. H. Su, J. H. Lin, W. H. Chen, Effect of multi micro porous layer in proton exchange membrane fuel cell, Exchange Membrane Fuel Cell (2010) 1-4.

[29]   L. R. Jordan, A. K. Shukla, T. Behrsing, N. R. Avery, B. C. Muddle, M. Forsyth, Journal of Power Sources 86 (2000) 250-254.

[30]   A. Tamayol, F. McGregor, M. Bahrami, Single phase through-plane permeability of carbon paper gas diffusion layers, J. Power Sources 204 (2012) 94-99.

Figures Captions

Fig. 1 A SEM cross-sectional image for the MPL coated (a) membrane filter and (b) carbon substrate.

Fig. 2 A schematic diagram of the experimental setup. Reprinted from Ref. [18] with the permission of Elsevier.

Fig. 3 A schematic diagram for the cross-section of the MPL-coated GDL.

Fig. 4 The values of the through-plane gas permeability of the MPLs for different carbon loadings. Reprinted from Ref. [17] with the permission of Elsevier.
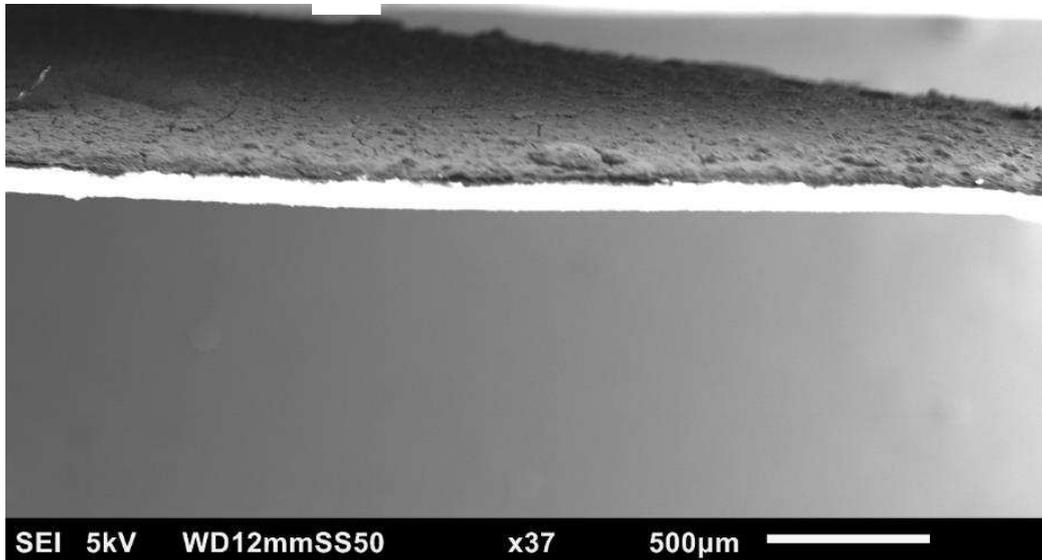
Fig. 5 A surface SEM images for an MPL-coated carbon substrate with 0.5 mg/cm^2 Ketjenblack carbon loading. Reprinted from [17] with permission from Elsevier.

Fig. 6 A surface SEM images for an MPL-coated carbon substrate with 2.0 mg/cm^2 Ketjenblack carbon loading. Reprinted from [17] with permission from Elsevier.

Fig. 7 A surface SEM image for an MPL-coated membrane filter with 0.5 mg/cm^2 Ketjenblack carbon loading.

Fig. 8 A typical surface SEM image for 10 BA carbon substrate.

Fig. 1

SEI   5kV   WD12mmSS50   x37   500µm

(a)

Acc.V Spot Magn   Det WD ┠────────────┨ 500 µm
20.0 kV 5.0   40x   SE   10.0 SGL 10BE
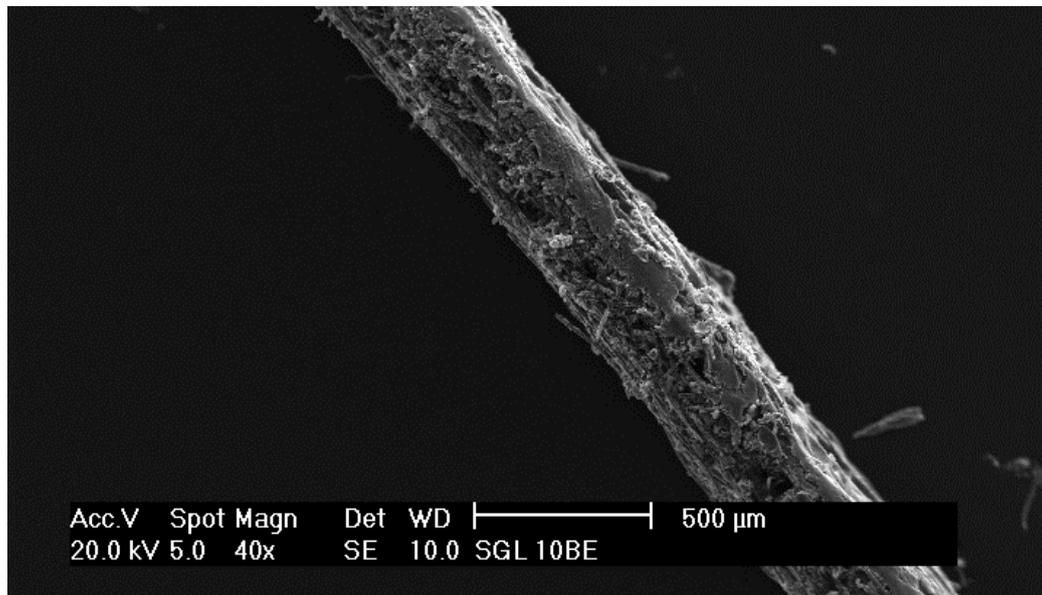
(b)

Fig. 2

Fig. 3

Fig. 4

Fig. 5

Fig. 6

Mag = 100 X   WD = 11.0 mm   20.00 kV   SE1   100 µm   LEMAS

Width = 3.009 mm

Fig. 7

Fig. 8

Mag = 100 X   WD = 10.0 mm   20.00 kV   SE1   100 µm   LEMAS
Width = 3.009 mm

24
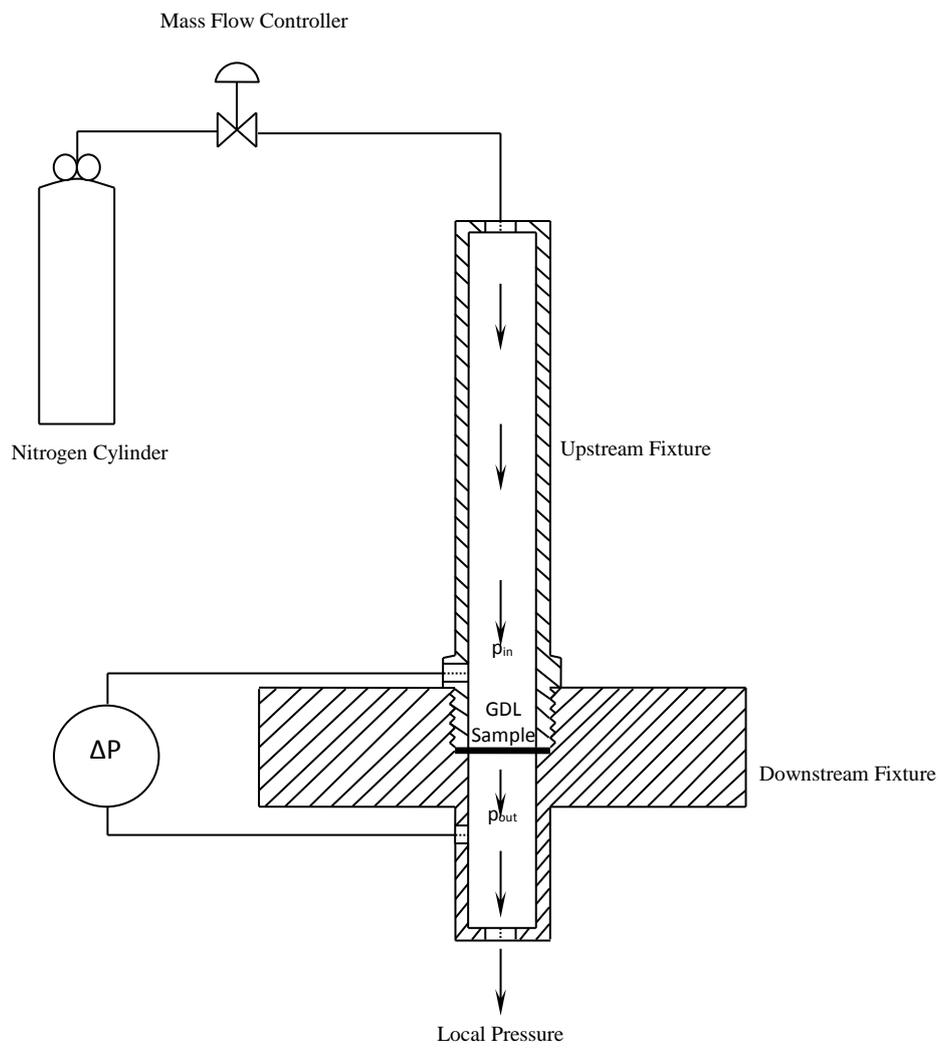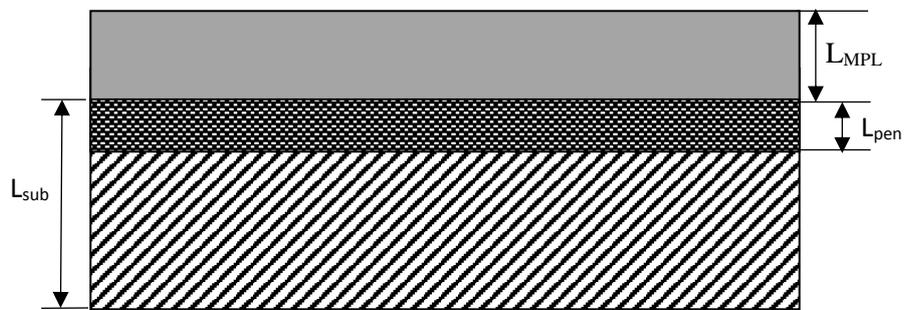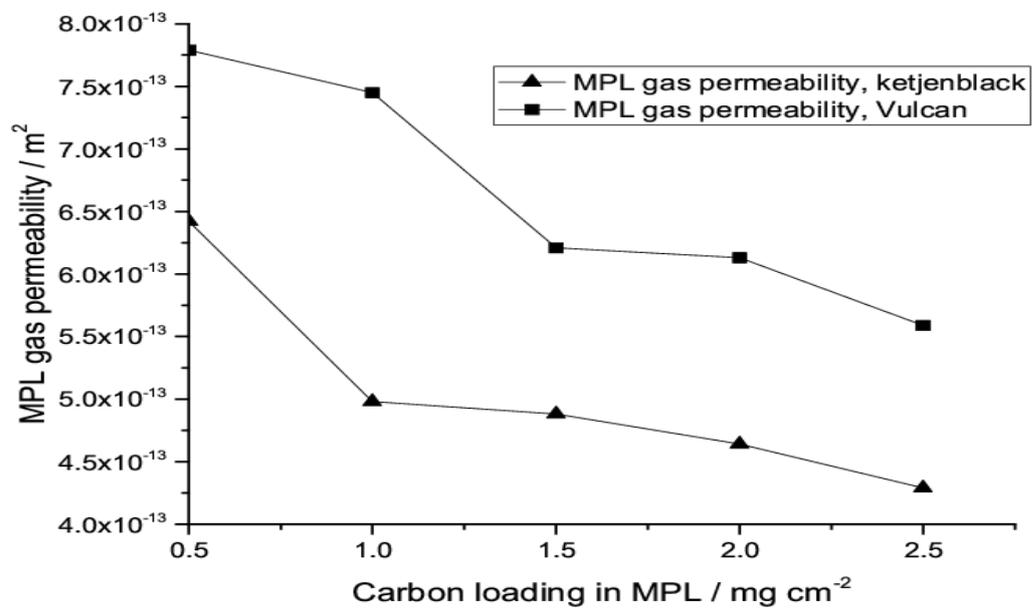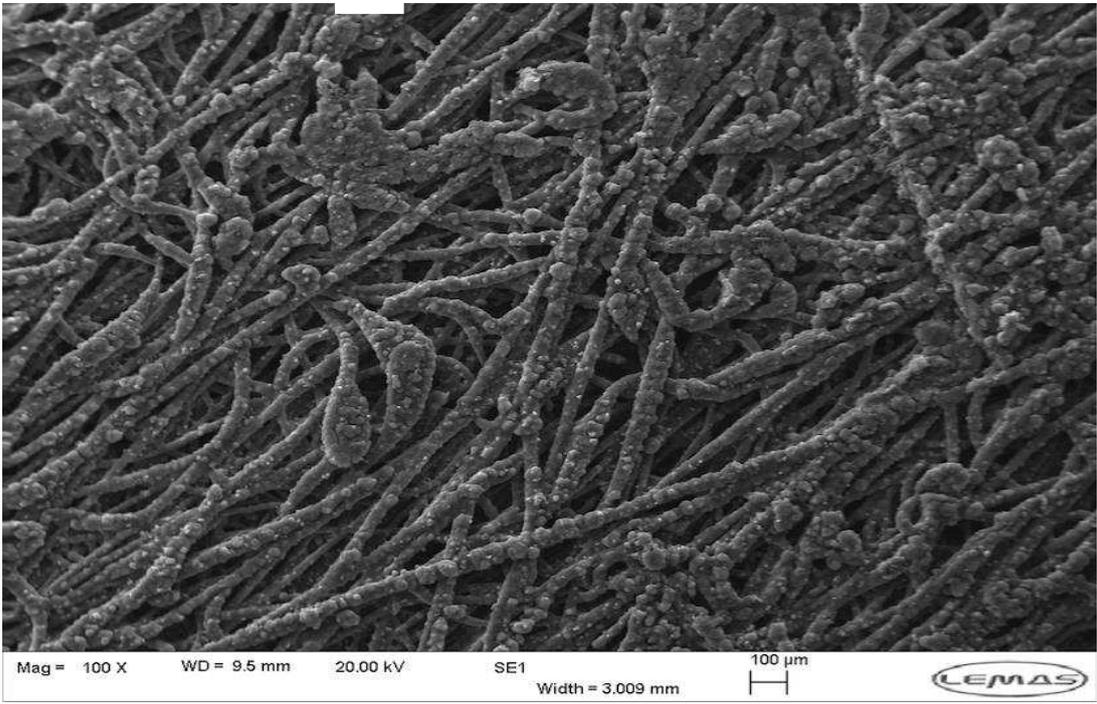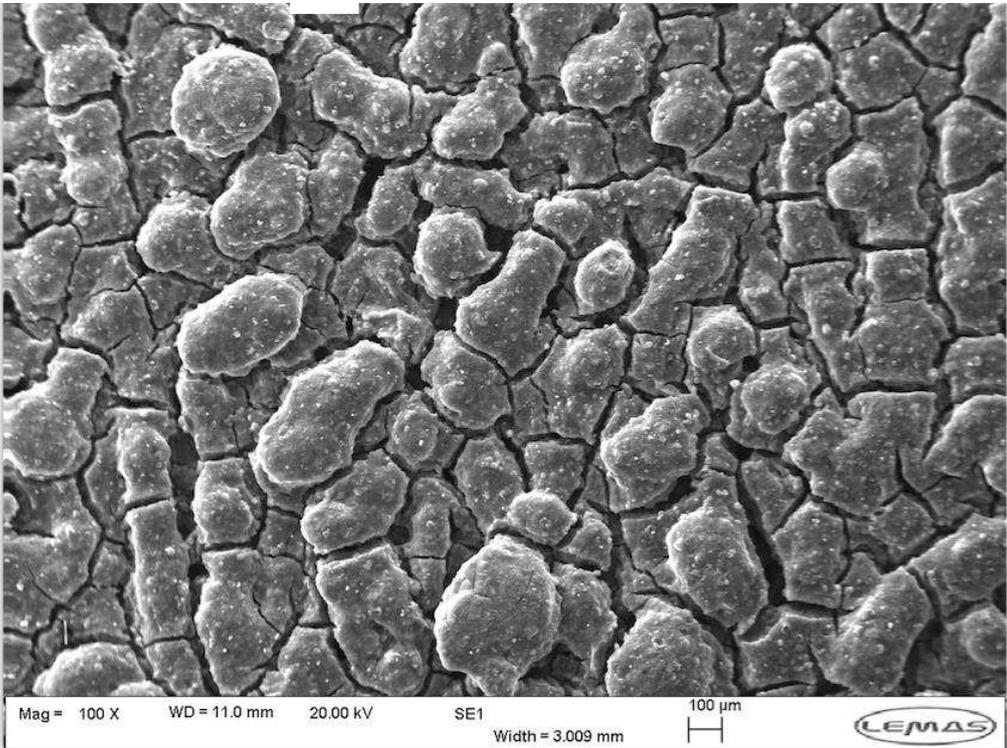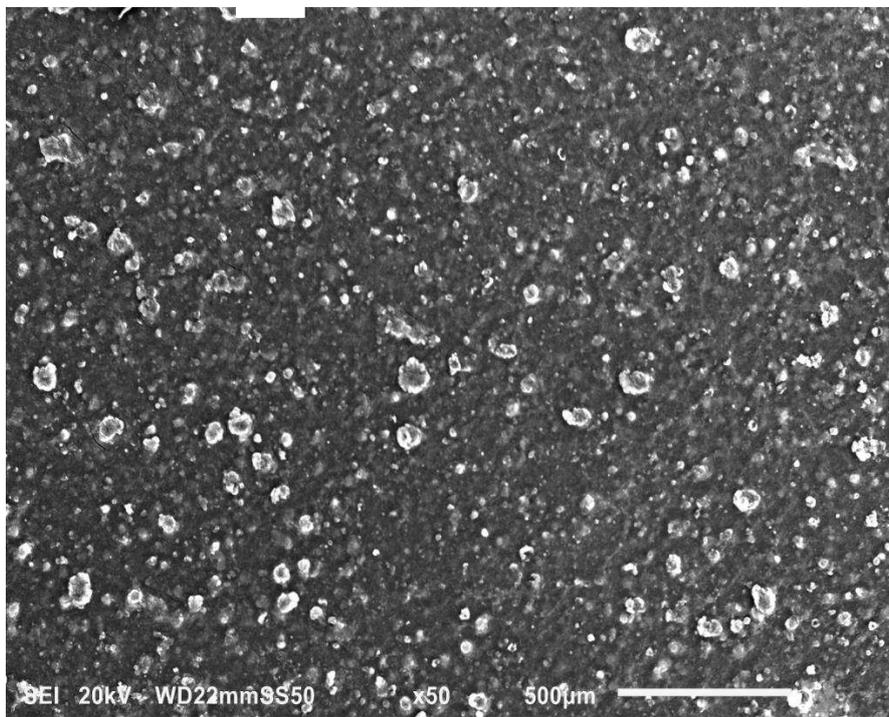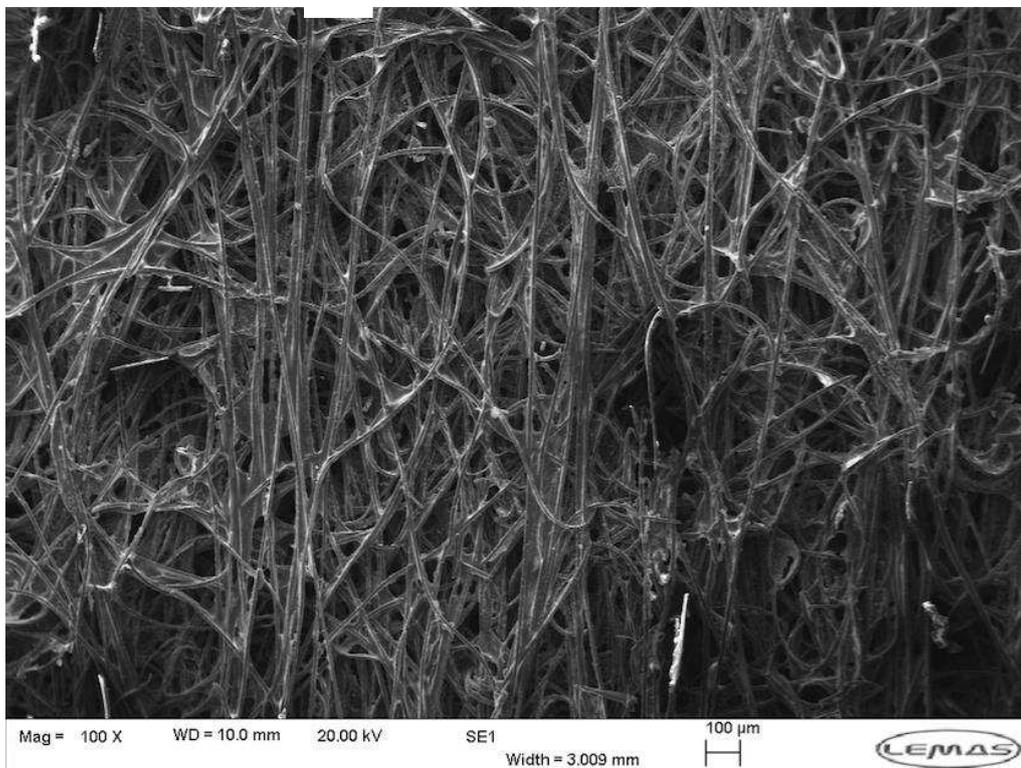
Table 1 Manufacturer's physical properties of the carbon blacks used.

Properties	Ketjenblack EC-300J	Vulcan XC-72R
Pore volume (ml/100 g)	310-345	178
Apparent bulk density (kg/m^3)	125-145	20-380
Surface area (m^2/g)	950	254
Particle diameter (nm)	30	30
pH	9.0-10.5	2-11
Volatile (by weight % max.)	1.0	2-8

Table 2 Manufacturer's physical properties of the SGL 10BA carbon paper substrate.

Physical parameter	Carbon substrate
Material	SGL 10BA
Thickness (μm)	380 ± 70
Porosity	0.88
PTFE loading (% by weight)	5

Table 3 - **The values of the parameters used to calculate the permeability of the MPL coating the carbon substrate with a Ketjenblack carbon loading of 2.0 mg/cm^2.**

Sample Number	$L_{tot} \times 10^{-4}$ (m)	$k_{tot} \times 10^{-12}$ (m^2)	$L_{sub} \times 10^{-4}$ (m)	$k_{sub} \times 10^{-11}$ (m^2)	$L_{MPL} \times 10^{-4}$ (m^2)	$K_{MPL} \times 10^{-13}$ (m^2)
1	4.75	2.34	3.60	1.84	1.15	6.27
2	4.70	2.15	3.60	1.98	1.10	5.49
3	4.85	1.78	3.25	2.09	1.16	6.23
4	4.44	2.54	3.43	1.88	1.30	6.45
5	4.55	1.98	3.25	1.69	1.30	6.17
6	4.23	2.50	3.24	2.69	1.10	6.81

Table 4 - **The values of the parameters used to calculate the permeability of the MPL coating the membrane filter. Note that single values were used for the permeability (3.72×10^{-13} m^2) and the thickness (1.40×10^{-4} m) of the membrane filter.**

Carbon black	Carbon loading (mg cm^{-2})	$L_{tot} \times 10^{-4}$ (m)	K_{tot} (m^2)	L_{MPL} (m)	K_{MPL} (m^2)
Ketjenblack	0.5	1.60	3.60×10^{-13}	2.00×10^{-5}	2.94×10^{-13}
	1.0	1.80	3.50×10^{-13}	4.00×10^{-5}	2.90×10^{-13}
Vulcan	0.5	1.46	2.83×10^{-13}	6.0×10^{-6}	4.29×10^{-14}
	1.0	1.52	2.32×10^{-13}	1.20×10^{-5}	4.30×10^{-14}